Research Article

BIOMEDICAL Journal of Scientific & Technical Research

ISSN: 2574 -1241

DOI: 10.26717/BJSTR.2021.37.006064

Cobalt Doped TiO_2/rGO Nanocomposites as Highly Efficient Photocatalyst for Water Purification

Xiuxiu Zhang[1,2,3], Guiyun Yi[1,2,3,4]*, Haiyang Fan[1,2,3], Peng Li[1,2,3], Zhengting Zhang[1,2,3], Yuanfeng Wu[1,2,3]*, Lunjian Chen[1,2,3], Chuanxiang Zhang[1,2,3], Yulong Zhang[1,2,3] and Qi Sun[1,2,3]

[1]*College of Chemistry and Chemical Engineering, Henan Polytechnic University, China*

[2]*Collaborative Innovation Center of Coal Work Safety of Henan Province, China*

[3]*Henan Key Laboratory of Coal Green Conversion, China*

[4]*State Collaborative Innovation Center of Coal Work Safety and Clean-efficiency Utilization, China*

ORCID: 0000-0002-8634-7931

***Corresponding authors:** Guiyun Yi, College of Chemistry and Chemical Engineering, Henan Polytechnic University, Collaborative Innovation Center of Coal Work Safety of Henan Province, Henan Key Laboratory of Coal Green Conversion, State Collaborative Innovation Center of Coal Work Safety and Clean-efficiency Utilization, Jiaozuo, 454003, China

Yuanfeng Wu, College of Chemistry and Chemical Engineering, Henan Polytechnic University, Collaborative Innovation Center of Coal Work Safety of Henan Province, Henan Key Laboratory of Coal Green Conversion, Jiaozuo, China

ARTICLE INFO

Received: July 09, 2021

Published: August 05, 2021

Citation: Xiuxiu Zhang, Guiyun Yi, Haiyang Fan, Peng Li, Yuanfeng Wu, et al., Cobalt Doped TiO_2/rGO Nanocomposites as Highly Efficient Photocatalyst for Water Purification. Biomed J Sci & Tech Res 37(5)-2021. BJSTR. MS.ID.006064.

Keywords: TiO_2; Cobalt-doping; GO; Photocatalysis

Abbreviations: TiO_2: Titanium Dioxide; GO: Graphene Oxide; MB: Methylene Blue; rGO: Reduced Graphene Oxide; CV: Crystal Violet; EIS: Electrochemical Impedance Spectroscopy; IPA: Isopropyl Alcohol; AO: Ammonium Oxalate; BQ: Benzoquinone

ABSTRACT

An efficient Co-TiO_2/rGO nanocomposite for photocatalytic degradation of organic dyes were successfully prepared by hydrothermal method with $Co(NO_3)_2 \cdot 6H_2O$, titanium dioxide (TiO_2) and graphene oxide (GO) as raw materials. The morphology and structure of the as-prepared materials were characterized by XRD, SEM, UV-Vis and XPS. Methylene blue (MB), a typical organic dye, was selected as the probe to investigate the effects of the mass ratio of GO and Co-TiO_2, the dosage amount of catalyst and the cycling performance of Co-TiO_2/rGO. The results showed that the band gap width of the prepared Co-TiO_2/rGO composite was about 2.92eV, and when the mass ratio of GO and Co-TiO_2 was 0.01 and the dosage was 20mg, the highest photocatalytic degradation of MB was observed with the degradation rate of 99.7%. Significantly, after 5 times of photocatalytic recycle was conducted, the degradation rate of MB by Co-TiO_2/rGO was still above 70%.

Highlights

i. The Cobalt doped TiO_2/rGO nanocomposites were prepared through a sample hydrothermal method.

ii. Compared with TiO_2, MB degradation percentage increased from 57.4% to 99.7% in the existence of Co-TiO_2/rGO-2.

iii. After 5 times of photocatalytic recycle performance tests, the degradation rate of MB by Co-TiO_2/rGO was still 78.2%.

Introduction

Photocatalysis is a crucial research filed, which solves the problem of energy and environmental pollution in the world in an economical and sustainable way [1]. Titanium dioxide (TiO_2), as the most common candidate among various semiconductor photocatalysts, has been widely utilized in the environmental filed because of its high activity, long-term stability and low toxicity [2-6]. However, because of its wide band gap (Eg≈3.2 eV for anatase type TiO_2) and high recombination rate of electron-hole pairs, TiO_2 can solely adsorb the UV light which is merely 3~5% of solar spectrum, resulting in low utilization of the majority of the solar energy [7-9]. In order to overcome these drawbacks, various improvement

methods have been explored including heterogenous composition [10,11], element doping [12,13], surface modification and the like. Among them, the element doping of TiO_2 photocatalysts has been considered as a feasible method to improve the interfacial charge-transfer efficiency, narrow the band gap and delay the recombination of carriers. Up to now, transition metal such as Co [14,15], Pt [16], Sn [17] and Fe [18] has been reported to be successfully doped into TiO_2, and the light response wavelength of the obtained materials showed significant red-shift. According to literatures, transition metals cobalt is considered as one of the best candidates to reduce the electron-hole recombination rate and transfer the adsorption edge to the visible light region [19-21]. The cobalt oxide-loaded TiO_2 (TiO_2-CoO) support with reduced graphene oxide (rGO) was fabricated by sol-gel method and utilized to remove 2-chlorophenol (2-CP).

The removal efficiency of 2-CP was 98.2% with the ternary nanocomposite in the visible region [22]. The ternary rGO-TiO_2/Co_3O_4 nanocomposites were successfully prepared by co-precipitation method, and exhibited the highest degradation performance of methylene blue (MB) and crystal violet (CV) dye under visible light [23]. As a result, cobalt doped TiO_2 photocatalysts have shown superior performance in degrading various organic pollutants. Graphene oxide (GO), due to its excellent electrical conductivity, large surface area and chemical stability, has attracted wide attention as a substrate for promoting the uniform distribution of heterojunction materials and enhancing the photocatalytic activity [24-28]. Due to the conjugated structure of GO, the nanocomposite of modified TiO_2 supported with graphene oxide were the perfect combination to enhance the charge separation during the electron-transfer processes. Therefore, the coupling of graphene oxide with some semiconductors has received particular attention in recent years [6]. In this paper, Cobalt doped TiO_2/rGO composites was successfully fabricated through hydrothermal method for MB degradation. The results demonstrated that the Co-TiO_2/rGO composites remarkably enhanced the MB degradation efficiency. Furthermore, recycling degradation experiments revealed excellent stability of the fabricated Co-TiO_2/rGO nanocomposites for treatment of target contaminant.

Materials and Methods

Materials

Cobalt nitrate hexahydrate ($Co(NO_3)_2 \cdot 6H_2O$, 98%), Tetrabutyl titanate ($C_{16}H_{36}O_4Ti$), glacial acetic acid ($C_2H_4O_2$), ethanol (C_2H_5OH) and macrogol 400 (HO (CH_2CH_2O) n H) were obtained from He Dong Hong Yan reagent factory of Tian Jin. Natural flake graphite (≥99.85%) was purchased from Sinopharm Chemical Reagent Co. Ltd.

Catalysts Synthesis

Co-TiO_2 catalysts were prepared by one-step hydrothermal method. In a typical synthesis procedure, 10mL tetrabutly titanate was dissolved in ethanol (20mL) to form homogenous solution "A", whereas 0.02g Co $(NO_3)_2 \cdot 6H_2O$ dissolved in a solution of ethyl alcohol, glacial acetic acid, macrogol 400 and deionized water to form solution "B". Subsequently, solution "A" was introduced into solution "B", and the obtained dispersion was heated at 180 °C for 5h. In following step, the prepared catalysts were washed by centrifugation with ethanol and dried at 80 °C. The obtained composites were light yellow particle and calcined in a muffle furnace at 500 °C for 3h, and the obtained sample was named as Co-TiO_2. The GO was synthesized by modified Hummers method. 20mg GO powder was dispersed in a solution of deionized water (40mL) and ethanol (20mL) through 30min ultrasonic, and then 200mg Co-TiO_2 was introduced to the GO suspension under vigorous stirring. Subsequently, the solution was heated at 140 °C for 5h. The resulting precipitate was washed with deionized water and dried at 80 °C. The final composites powders were labelled as Co-TiO_2/rGO-2. For comparison, the samples prepared by adding 10mg, 30mg GO powder were denoted as Co-TiO_2/rGO-1 and Co-TiO_2/rGO-3, respectively.

Characterization Methods

The purity and crystallinity of the prepared samples were collected by Bruker D8 Advance X-ray diffraction (Germany) with Cu Kα radiation. The morphology of the photocatalysts was characterized via Scanning electron microscope (Hitachi SU-4800). The Ultraviolet-Visible (UV-Vis) diffuse reflectance spectra (DRS) were implemented by using UV-3600 Plus. X-ray photoelectron spectroscopy (XPS) were obtained by ESCALAB 250XI (ThermoFischer Electron Corporation, USA). Electrochemical measurements were carried out on CHI 660E electrochemical workstation.

Photocatalytic Degradation

The photocatalytic efficiency of Co-TiO_2/rGO samples was investigated with MB degradation under visible light. The visible light source was Perfect 300W Xe-lamp (with a 420nm cut-off filter). In each experiment, 20mg of Co-TiO_2/rGO composite were added to 150mL MB solution (20mg/L). The suspension was stirred in the dark for 60min to ensure the attainment of adsorption-desorption equilibrium. 5mL sample solution was extracted at predetermined time and analyzed by UV-3600 plus. The removal efficiency (R) of MB was calculated by Eq. (1).

$$R = \left(\frac{(C_t - C_0)}{C_0} \right) \times 100 \quad (1)$$

It was expected that the degradation of the MB obeyed the pseudo-first-order reaction kinetics as follows:

$$Ln = (C_t / C_0) = -kt \quad (2)$$

where C_0 (mg/L) was the initial concentration of MB, C_t (mg/L) was the concentration of MB at time t, k was the kinetic constant.

Results and Discussion

Structure Characterization

Figure 1 were the XRD patterns of the as-prepared nanocomposites. It was clear that all samples exhibit similar diffraction peaks. The peaks located at 2θ = 25.34°, 37.85°, 47.99°, 54.04°, 62.67°, 68.79°, 70.31°, 75.05° and 82.49°, which could be indexed to (1 0 1), (0 0 4), (2 0 0), (1 0 5), (2 0 4), (1 1 6), (2 2 0), (2 1 5) and (2 2 4) planes of anatase TiO_2, demonstrating the high purity and good crystallinity of the samples [29]. The diffraction peaks of Co were not observed, which might be owing to the low content of Co $(NO_3)_2 \cdot 6H_2O$ or the cobalt ions were uniformly dispersed into the anatase crystallites. It was noteworthy that the peak intensity corresponding to the (2 1 1) crystal plane in the cobalt-doped nanocomposites varied, indicating that the presence of Co^{2+} ions around Ti^{4+} [30]. No significant diffraction peaks were noticed for XRD patterns of Co-TiO_2/rGO nanocomposites when compared with Co-TiO_2 nanoparticles, which was described the low rGO content in the composite, or of the TiO_2 loading on the rGO surface [31,32]. Surface morphology of the as-prepared composites was assayed through SEM analyses. It could be seen from Figure 2a that the Co-TiO_2 particles were subsphaeroidal and well-dispersed. Figure 2b showed that the agglomeration occurred when subsphaeroidal Co-TiO_2 particles were combined with graphene sheets. The element composition of the Co-TiO_2/rGO-2 nanocomposites were confirmed by EDS analysis. In the element mapping images (Figures 2c & 2d), C, Ti, O and Co disperse uniformly in the selected area of Co-TiO_2/rGO-2, suggesting that cobalt atoms were successfully doped into the composites. According to these images, the cobalt atoms were evenly distributed in TiO_2 particles, indicating that the interaction between cobalt and TiO_2 particles was excellent in the hydrothermal synthesis procedure [15].

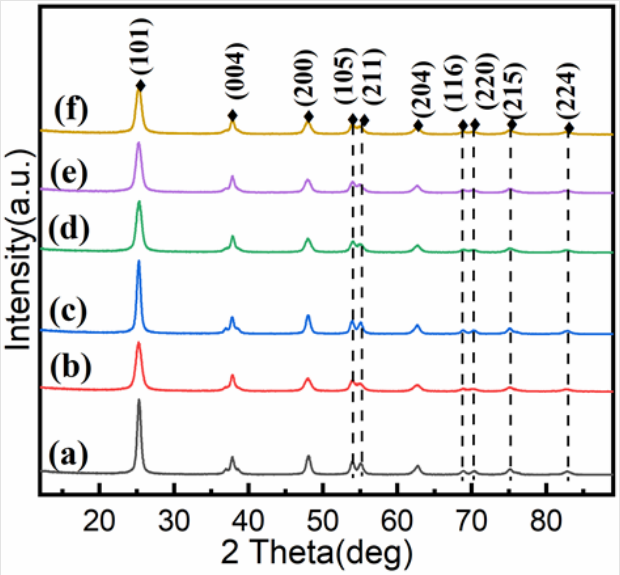

Figure 1: XRD patterns of

a) TiO_2;

b) Co-TiO_2;

c) TiO_2/rGO;

d) Co-TiO_2/rGO-1;

e) Co-TiO_2/rGO-2;

f) Co-TiO_2/rGO-3

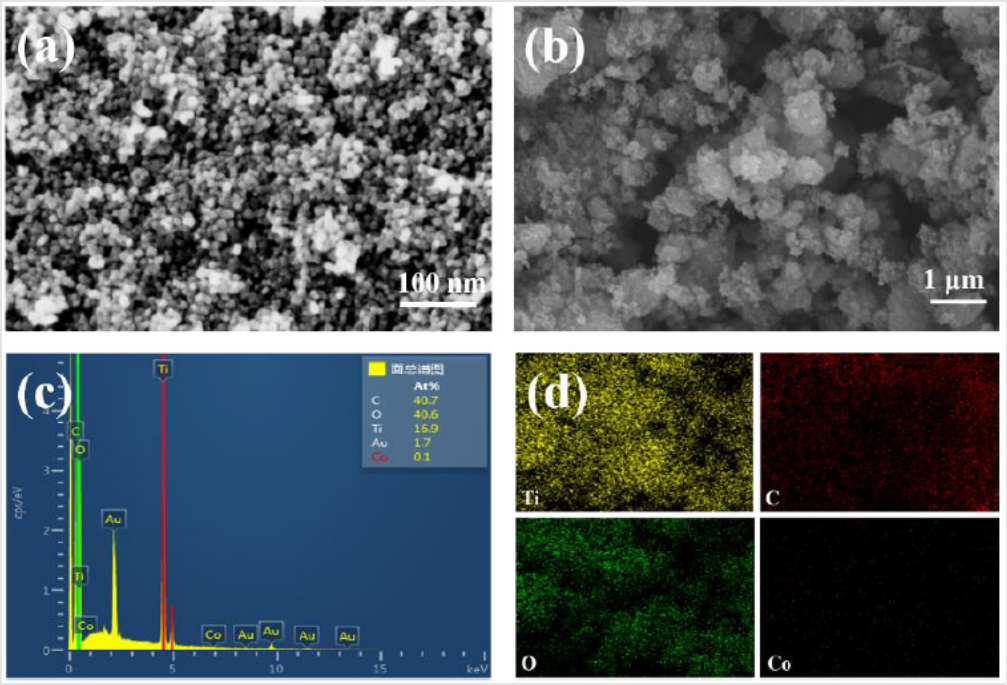

Figure 2: SEM images of
a) TiO_2;
b) Co-TiO_2/rGO-2;
c) C and
d) EDS analysis of Co-TiO_2/rGO-2.

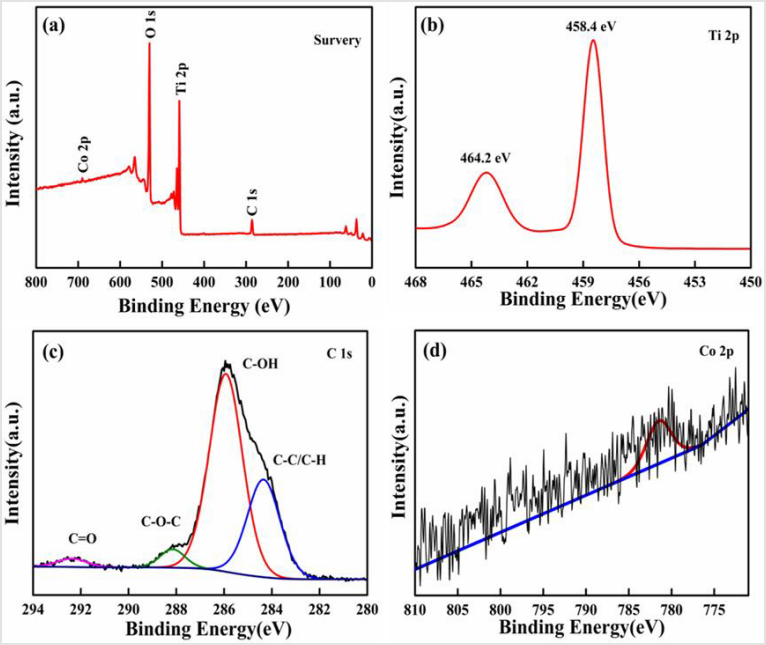

Figure 3:
a) Full XPS spectrum and high-resolution spectrum of
b) Ti 2p
c) C1s and
d) Co 2p

The chemical oxidation state of Co-TiO_2/rGO-2 nanocomposites were measured by XPS analysis (Figure 3). As shown in Figure 3a, the XPS survey spectrum of the Co-TiO_2/rGO-2 presented that C, O, Ti and Co elements could be revealed, which could consistent well with the result of EDS element mapping. The spectrum of Ti 2p (Figure 3b) exhibited two main peaks at 464.2 and 458.4eV, which were assigned to the Ti $2p_{1/2}$ and Ti $2p_{3/2}$ [33]. The C 1s spectrum of Co-TiO_2/rGO-2 composite was fitted into four peaks at 292.3eV, 288.1eV, 285.9eV and 284.3eV, which were signed to C= O, C= O= C, C= OH and C= C/C= H, respectively [34,35]. In the Co 2p core level of the Co-TiO_2/rGO-2 nanocomposites (Figure 3d), the peak appearing at 781.2 eV corresponded to Co (II) ions [36,37]. The optical property of TiO_2 and Co-TiO_2/rGO was inspected by UV-Vis adsorption spectra, as displayed in Figures 4a & 4b. Pure TiO_2, with equal to 3.18eV and adsorption edge at 390nm, showed almost no visible light adsorption. Compared with the adsorption edge of pure TiO_2, a strong light adsorption intensity at approximately 430nm was observed for the Co-TiO_2/rGO-2 composites, which was associated to the formation of Ti-O-C bonds, resulting in reduced excited photons energies and hence low band gap energy [38]. As a result, the visible light adsorption efficiency of Co-TiO_2/rGO-2 can be effectively enhanced due to the cobalt cations and rGO, which is beneficial to improving the photocatalytic degradation activity.

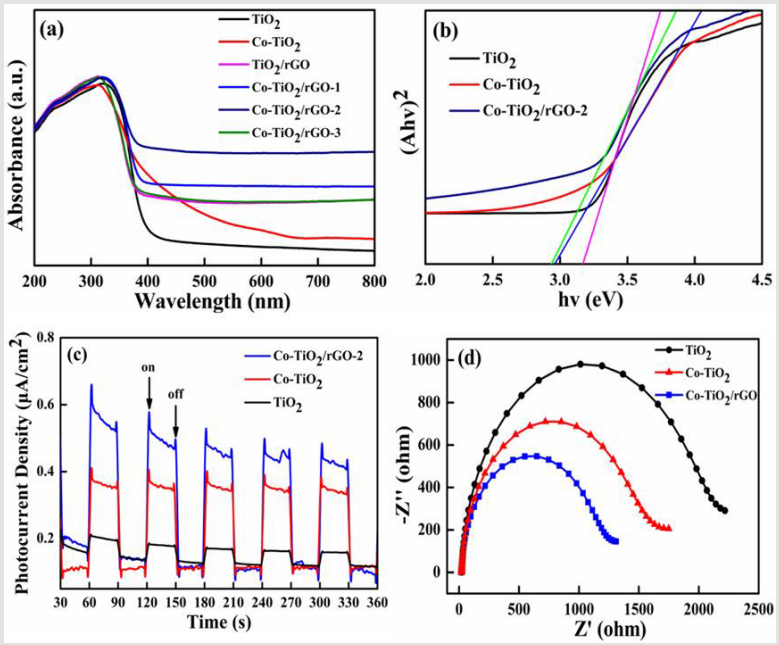

Figure 4:

a) UV-Vis diffuse reflectance spectra of TiO_2, Co-TiO_2, TiO_2/rGO and Co-TiO_2/rGO;

b) Plot of Kubelka-Munk function versus band gap energy of TiO_2, Co-TiO_2 and Co-TiO_2/rGO-2;

c) The transient photocurrent density of TiO_2, Co-TiO_2 and Co-TiO_2/rGO-2;

d) Electrochemical impedance spectra of Nyquist plots of TiO_2, Co-TiO_2 and Co-TiO_2/rGO-2.

In order to reveal the behaviors of charge transfer and separation in the prepared photocatalysts, the photocurrent response and electrochemical impedance spectroscopy (EIS) were recorded [39]. Figure 4c showed the transient photocurrent responses of TiO_2, Co-TiO_2 and Co-TiO_2/rGO-2 composites. It could be found that the photocurrent densities of Co-TiO_2/rGO-2 composites were significantly higher than that those of other samples, implying the efficient separation efficiency of electron-hole pairs. Figure 4d exhibited EIS changes of TiO_2, Co-TiO_2 and Co-TiO_2/rGO-2 composites. It was clearly observed that the Co-TiO_2/rGO-2 possessed much smaller arc radius relative to TiO_2 and Co-TiO_2, indicating that Co-TiO_2/rGO-2 had lower resistance and faster separation of electron-hole in the charge transfer processes, which could well correspond to the photocurrent results.

Photocatalytic Performances

The photocatalytic performances of the TiO_2, Co-TiO_2, TiO_2/rGO and Co-TiO_2/rGO composites were evaluated by degradation MB. As exhibited in Figure 5a, the Co-TiO_2/rGO-2 nanocomposites had the highest photocatalytic performance. For pure TiO_2 nanoparticles, only 57.4 % of the MB was removed following 210 min under visible light irradiation. Nonetheless, the removal percentage of MB

by TiO_2/rGO and Co-TiO_2/rGO-2 nanocomposites was 83.5% and 99.7%, respectively. The enhanced activity of the Co-TiO_2/rGO-2 nanocomposites might have been attributed to the introduction of Co ions and rGO. Figure 5b manifested the kinetic constant (k) of the as-prepared photocatalytic. The k value of pure TiO_2 and TiO_2/rGO were 0.0025 and 0.0063 min^{-1}, respectively. While the Co-TiO_2/rGO-2 nanocomposites exhibited the highest MB photodegradation rate (0.0125 min^{-1}), which was almost 5 and 1.98 times faster than those of the TiO_2 and TiO_2/rGO, respectively. To identify the optimum dosage of the photocatalyst, a series of experiments were carried out by varying the concentration of catalyst from 10mg to 40mg in 150mL of MB (20mg/L) (Figure 5c). It was realized that the removal efficiency of MB increased from 69.3% to 99.7% with the Co-TiO_2/rGO-2 nanocomposites increased from 10mg to 20mg, which was ascribed to the availability of enough active sites on the catalyst surface. Whereas the remove efficiency decreased with a further increase in the Co-TiO_2/rGO-2 dosage, which was ascribed to the agglomeration of the photocatalyst. Based on the above results, the optimal dosage of Co-TiO_2/rGO-2 nanocomposites for MB degradation was to be 20mg. The stability and recyclability of the photocatalyst exerts great impact on the operating cost of wastewater treatment. Therefore, the stability of the photocatalysts was evaluated for the Co-TiO_2/rGO-2 nanocomposites and the results were showed in Figure 5c. The study indicated that the removal efficiency of MB was still 78.2% after five recycling runs, indicating the activity of the recovered Co-TiO_2/rGO-2 was stable enough for recycling. Therefore, Co-TiO_2/rGO-2 nanocomposites were expected to be promising in environmental remediation because of their excellent photocatalytic activity and stability.

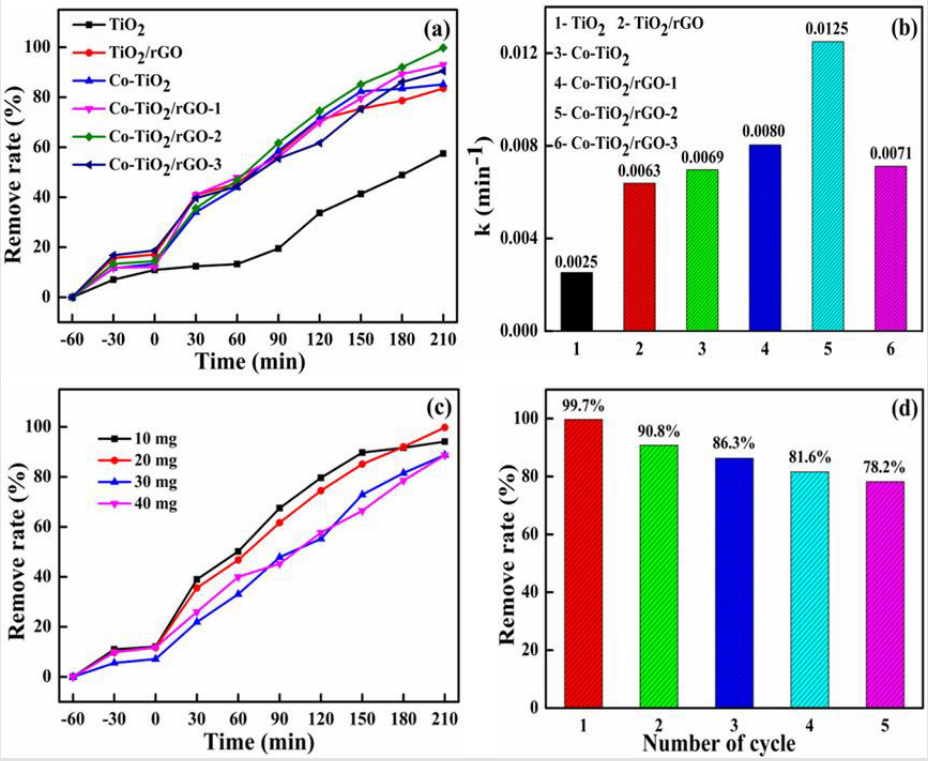

Figure 5:

a) Photodegradation of MB under simulated solar irradiation over the as-prepared photocatalytic;

b) The kinetic constants of the as-prepared photocatalytic for the MB photodegradation;

c) Efficient of the dosage of the MB photodegradation by Co-TiO_2/rGO-2;

d) Effect of cycling times on photocatalytic efficiency on Co-TiO_2/rGO-2

Proposed Mechanism for Photocatalytic Degradation of MB

To determine the active species (such as •OH or h^+ or $•O_2^-$ radicals) and further explore the photodegradation mechanism, isopropyl alcohol (IPA), ammonium oxalate (AO) and 1,4-benzoquinone (BQ) were used as the radical scavengers [40,41]. The experiment data revealed that the photocatalytic activity of Co-TiO_2/rGO-2 was decreased by adding the radical scavengers but to different degrees (Figure 6), indicating that all the above active radical species were responsible for the MB degradation. Notably, the photocatalytic performance dropped sharply to 61.1% with the addition of IPA, demonstrating that h^+ radical was the main active species in the

MB degradation process. Based on the above characterization and photocatalytic activity results, a plausible mechanism of Co-TiO_2/rGO-2 for MB degradation has been proposed and shown in Figure 7. The improvement of TiO_2 photocatalytic performance could be explained as follows:

1) The doping of optimal Co^{2+} into the lattice of TiO_2 nanosheet could efficiently reduce the band gap width of TiO_2 and increase the adsorption of visible light [42,43].

2) The specific surface area of the composite increased due to adding rGO, and more active sites could be provided for photocatalytic activity [44].

3) Under the excitation of visible light, the electrons generated by the conduction band of TiO_2 were captured and transferred by the graphene layer, which improved the electron-holes separation efficiency [45,46].

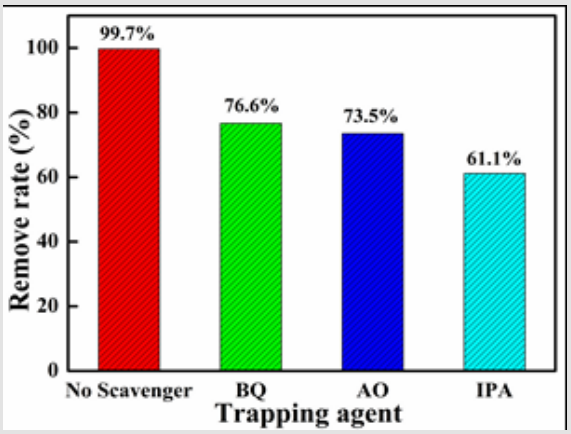

Figure 6: Effects of radical scavengers on the degradation of MB over Co-TiO_2/rGO-2 nanocomposite.

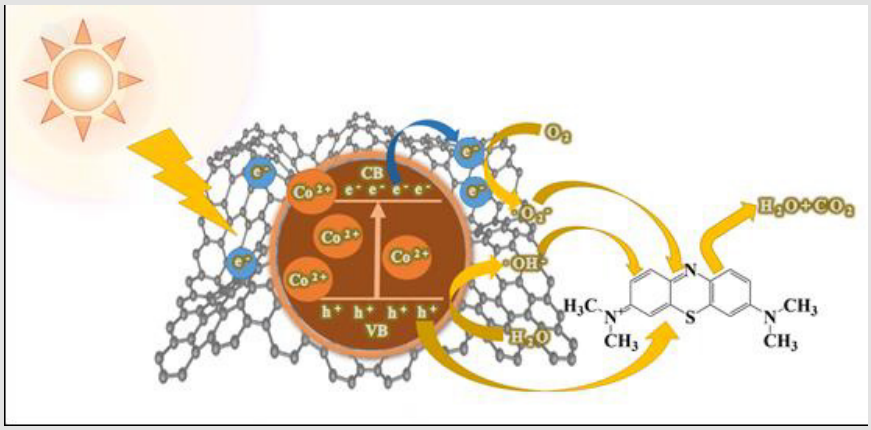

Figure 7: The probable photocatalytic degradation mechanism for MB by the Co-TiO_2/rGO nanocomposites.

The electrons subsequently react with the oxygen molecules adsorbed on the surface of the catalyst to generate $\bullet O_2^-$ to degrade MB. At the same time, the residual h^+ within the TiO_2 VB can be directly or through water oxidation to generate ·OH radicals, and in turn photo oxidize of MB [15]. In summary, the addition of Co metals to TiO_2/reduced graphene oxide composite have demonstrated to be beneficial for degrading MB, which was consistent with the electrochemical measurements. The synergy effects of Cobalt doped TiO_2 and rGO was conducive to the formation of the active sites and the facilitation of the high photocatalytic performance. Therefore, Co-TiO_2/rGO composite offered an excellent combination of high activity and long-term performance durability.

Conclusion

In conclusion, an efficient Cobalt doped TiO_2/rGO photocatalyst was successfully prepared, and the properties of Co-TiO_2/rGO nanocomposites were investigated. It was noticed that the Co-TiO_2/rGO-2 revealed an excellent photocatalytic performance in the MB degradation process. Compared to TiO_2, MB degradation percentage was increased from 57.4% to 99.7% in the existence of Co-TiO_2/rGO-2. This phenomenon could be explained as the special properties of reduced graphene oxide components and cobalt dopant, which facilitate the separation of photo-generated carries and extend the adsorption spectrum of TiO_2 into visible region. Furthermore, the

degradation percentage of MB was still obtained to 78.2% after five cycles. Therefore, Co-TiO_2/rGO nanocomposites have promising applications in degradation of the organic compounds in the coloring, petroleum and leather industries.

Acknowledgment

This work was supported by the National Key Research Plan (2018YFB0604500), the National Natural Science Foundation of China (U1803114), the Key Scientific and Technological Project of Henan Province (202102210183), the China Postdoctoral Science Foundation (207500), Outstanding Foreign Scientists Studio of Coal Green Conversion of Henan Province (GZS2020012), National Natural Science Foundation of China (51974110) and the Program for Science & Technology Innovation Talents in Universities of Henan Province (21HASTIT008).

References

1. NT Padmanabhan, N Thomas, J Louis, DT Mathew, P Ganguly, et al. (2021) Graphene coupled TiO_2 photocatalysts for environmental applications: A review. Chemosphere 271: 129506.
2. X Zhang, Y Yu, D Jiang, Y Jiao, Y Wu, et al. (2019) Synthesis and characterization of a bi-functional hydroxyapatite/Cu-doped TiO_2 composite coating. Ceramics International 45(6): 6693-6701.
3. X Zhang, Z Peng, X Lu, Y Lv, G Cai, et al. (2020) Microstructural evolution and biological performance of Cu-incorporated TiO_2 coating fabricated through one-step micro-arc oxidation. Applied Surface Science 508: 144766.
4. X Zhang, Y Wu, Y Lv, Y Yu, Z Dong (2020) Formation mechanism, corrosion behaviour and biological property of hydroxyapatite/TiO_2 coatings fabricated by plasma electrolytic oxidation, Surface and Coatings Technology 386: 125483.
5. J Guo, Y Li, S Li, X Cui, Y Liu, et al. (2020) One-step fabrication of TiO_2/graphene hybrid mesoporous film with enhanced photocatalytic activity and photovoltaic performance. Chinese Journal of Catalysis 41(8): 1208-1216.
6. H Fan, G Yi, X Zhang, B Xing, C Zhang, et al. (2021) Facile synthesis of uniformly loaded Fe_3O_4-TiO_2/RGO ternary hybrids for enhanced photocatalytic activities. Optical Materials 111: 110582.
7. L Elsellami, F Dappozze, N Fessi, A Houas, C Guillard (2018) Highly photocatalytic activity of nanocrystalline TiO_2 (anatase, rutile) powders prepared from $TiCl_4$ by sol–gel method in aqueous solutions. Process Safety and Environmental Protection 113: 109-121.
8. A Fujishima, X Zhang, D Tryk (2008) TiO_2 photocatalysis and related surface phenomena. Surface Science Reports 63(12): 515-582.
9. Q Guo, C Zhou, Z Ma, X Yang (2019) Fundamentals of TiO2 Photocatalysis: Concepts, Mechanisms, and Challenges. Adv Mater 31(50): e1901997.
10. CH Nguyen, ML Tran, TTV Tran, RS Juang (2020) Enhanced removal of various dyes from aqueous solutions by UV and simulated solar photocatalysis over TiO_2/ZnO/rGO composites. Separation and Purification Technology 232: 115962.
11. C Park, T Ghosh, Z Meng, U Kefayat, N Vikram, et al. (2013) Preparation of CuS-graphene oxide/TiO_2 composites designed for high photonic effect and photocatalytic activity under visible light. Chinese Journal of Catalysis 34(4): 711-717.
12. T Barkhade, I Banerjee (2019) Optical Properties of Fe doped TiO_2 Nanocomposites Synthesized by Sol-Gel Technique. Materials Today: Proceedings 18(3): 1204-1209.
13. Y Li, R Fu, M Gao, X Wang (2019) B–N co-doped black TiO_2 synthesized via magnesiothermic reduction for enhanced photocatalytic hydrogen production. International Journal of Hydrogen Energy 44(54): 28629-28637.
14. WK Jo, S Kumar, MA Isaacs, AF Lee, S Karthikeyan (2017) Cobalt promoted TiO_2/GO for the photocatalytic degradation of oxytetracycline and Congo Red. Applied Catalysis B: Environmental 201(10): 159-168.
15. S Jamali Alyani, A Ebrahimian Pirbazari, F Esmaeili Khalilsaraei, N Asasian Kolur, N Gilani (2019) Growing Co-doped TiO_2 nanosheets on reduced graphene oxide for efficient photocatalytic removal of tetracycline antibiotic from aqueous solution and modeling the process by artificial neural network. Journal of Alloys and Compounds 799: 169-182.
16. ZY Zhao (2014) Theoretical Study of Pt Cocatalyst Loading on Anatase TiO_2(101) Surface: From Surface Doping to Interface Forming. The Journal of Physical Chemistry C 118(42): 24591-24602.
17. M Xu, P Da, H Wu, D Zhao, G Zheng (2012) Controlled Sn-doping in TiO_2 nanowire photoanodes with enhanced photoelectrochemical conversion. Nano Lett 12(3): 1503-1508.
18. J Shi, G Chen, G Zeng, A Chen, K He, et al. (2018) Hydrothermal synthesis of graphene wrapped Fe-doped TiO_2 nanospheres with high photocatalysis performance. Ceramics International 44(2018): 7473-7480.
19. C Cao, C Hu, W Shen, S Wang, J Wang, et al. (2013) Fabrication of a novel heterostructure of Co3O4-modified TiO_2 nanorod arrays and its enhanced photoelectrochemical property. Journal of Alloys and Compounds 550: 137-143.
20. A Kaushik, B Dalela, S Kumar, PA Alvi, S Dalela (2013) Role of Co doping on structural, optical and magnetic properties of TiO_2. Journal of Alloys and Compounds 552: 274-278.
21. H Fan, G Yi, Q Tian, X Zhang, B Xing, et al. (2020) Hydrothermal-template synthesis and electrochemical properties of Co_3O_4/nitrogen-doped hemisphere-porous graphene composites with 3D heterogeneous structure. RSC Advances 10: 36794-36805.
22. A Sharma, BK Lee (2016) Rapid photo-degradation of 2-chlorophenol under visible light irradiation using cobalt oxide-loaded TiO_2/reduced graphene oxide nanocomposite from aqueous media. J Environ Manage 165: 1-10.
23. R Ranjith, V Renganathan, SM Chen, NS Selvan, PS Rajam (2019) Green synthesis of reduced graphene oxide supported TiO_2/Co_3O_4 nanocomposite for photocatalytic degradation of methylene blue and crystal violet. Ceramics International 45(10): 12926-12933.
24. Y Shen, Q Fang, B Chen (2015) Environmental applications of three-dimensional graphene-based macrostructures: adsorption, transformation, and detection. Environ Sci Technol 49(1): 67-84.
25. TF Yeh, J Cihlář, CY Chang, C Cheng, H Teng (2013) Roles of graphene oxide in photocatalytic water splitting. Materials Today 16(3): 78-84.
26. Y Shen, B Chen (2015) Sulfonated graphene nanosheets as a superb adsorbent for various environmental pollutants in water. Environ Sci Technol 49(12): 7364-7372.
27. G Yi, P Li, B Xing, Q Tian, X Zhang, et al. (2021) Nitrogen-rich graphene aerogel with interconnected thousand-layer pancake structure as anode for high performance of lithium-ion batteries. Journal of Solid State Chemistry 294: 121859.
28. X Zhang, G Yi, Z Zhang, J Yu, H Fan, et al. (2021) Magnetic graphene-based nanocomposites as highly efficient absorbents for Cr(VI) removal from wastewater. Environ Sci Pollut Res Int 28(12): 14671-14680.
29. L Zhang, C Ni, H Jiu, C Xie, J Yan, et al. (2007) One-pot synthesis of Ag-TiO_2 /reduced graphene oxide nanocomposite for high performance of adsorption and photocatalysis. Ceramics International 43(7): 5450-5456.

30. A Chanda, K Rout, M Vasundhara, SR Joshi, J Singh (2018) Structural and magnetic study of undoped and cobalt doped TiO_2 nanoparticle. RSC Advances 8: 10939-10947.

31. NM El Shafai, ME El Khouly, M El Kemary, MS Ramadan, AS Derbalah, et al. (2019) Fabrication and characterization of graphene oxide-titanium dioxide nanocomposite for degradation of some toxic insecticides. Journal of Industrial and Engineering Chemistry 69: 315-323.

32. I Tismanar, AC Obreja, O Buiu, A Duta (2021) VIS-active TiO_2 - graphene oxide composite thin films for photocatalytic applications. Applied Surface Science 538.

33. W Wang, D Xu, B Cheng, J Yu, C Jiang (2017) Hybrid carbon@TiO_2 hollow spheres with enhanced photocatalytic CO_2 reduction activity. Journal of Materials Chemistry A 5: 5020-5029.

34. H Hu, Z Zhao, W Wan, Y Gogotsi, J Qiu (2013) Ultralight and highly compressible graphene aerogels. Adv Mater 25(15): 2219-2223.

35. S Pu, R Zhu, H Ma, D Deng, X Pei, et al. (2017) Facile in-situ design strategy to disperse TiO_2 nanoparticles on graphene for the enhanced photocatalytic degradation of rhodamine 6G. Applied Catalysis B: Environmental 218: 208-219.

36. W Liu, L Cao, W Cheng, Y Cao, X Liu, et al. (2017) Single-Site Active Cobalt-Based Photocatalyst with a Long Carrier Lifetime for Spontaneous Overall Water Splitting. Angew Chem Int Ed Engl 56(32): 9312-9317.

37. H Fei, J Dong, MJ Arellano Jimenez, G Ye, N Dong Kim, et al. (2015) Atomic cobalt on nitrogen-doped graphene for hydrogen generation. Nat Commun 6: 8668.

38. J Tian, Z Zhao, A Kumar, RI Boughton, H Liu (2014) Recent progress in design, synthesis, and applications of one-dimensional TiO_2 nanostructured surface heterostructures: a review. Chem Soc Rev 43: 6920-6937.

39. J Li, W Zhao, F Huang, A Manivannan, N Wu (2011) Single-crystalline $Ni(OH)_2$ and NiO nanoplatelet arrays as supercapacitor electrodes. Nanoscale 12(3): 5103-5109.

40. WK Jo, T Sivakumar Natarajan (2015) Facile Synthesis of Novel Redox-Mediator-free Direct Z-Scheme $CaIn_2S_4$ Marigold-Flower-like/TiO_2 Photocatalysts with Superior Photocatalytic Efficiency. ACS Appl Mater Interfaces 7(31): 17138-17154.

41. WK Jo, TS Natarajan (2015) Influence of TiO_2 morphology on the photocatalytic efficiency of direct Z-scheme g-C_3N_4/TiO_2 photocatalysts for isoniazid degradation. Chemical Engineering Journal 281: 549-565.

42. P Jiang, W Xiang, J Kuang, W Liu, W Cao (2015) Effect of cobalt doping on the electronic, optical and photocatalytic properties of TiO_2. Solid State Sciences 46: 27-32.

43. M Iwasaki, M Hara, H Kawada, H Tada, S Ito (2000) Cobalt Ion-Doped TiO_2 Photocatalyst Response to Visible Light. J Colloid Interface Sci 224(1): 202-204.

44. W Wang, Z Wang, J Liu, Z Luo, SL Suib, et al. (2017) Single-step One-pot Synthesis of TiO_2 Nanosheets Doped with Sulfur on Reduced Graphene Oxide with Enhanced Photocatalytic Activity. Sci Rep 7: 46610.

45. L Zou, Y Qiao, XS Wu, CX Ma, X Li, et al. (2015) Synergistic effect of titanium dioxide nanocrystal/reduced graphene oxide hybrid on enhancement of microbial electrocatalysis. Journal of Power Sources 276: 208-214.

46. J Liu, Z Wang, L Liu, W Chen (2011) Reduced graphene oxide as capturer of dyes and electrons during photocatalysis: surface wrapping and capture promoted efficiency. Phys Chem Chem Phys 13(29): 13216-13221.

ISSN: 2574-1241

DOI: 10.26717/BJSTR.2021.37.006064

Guiyun Yi, Yuanfeng Wu. Biomed J Sci & Tech Res

Submission Link: https://biomedres.us/submit-manuscript.php